processes

MDPI

*Article*

# Fast History Matching and Flow Channel Identification for Polymer Flooding Reservoir with a Physics-Based Data-Driven Model

**Zhijie Wei [1,2], Yongzheng Cui [1,2,*], Yanchun Su [1,2] and Wensheng Zhou [1,2]**

[1] State Key Laboratory of Offshore Oil and Gas Exploitation, Beijing 102299, China; petroweizj@126.com (Z.W.); suych@cnooc.com.cn (Y.S.); wenshzhou@126.com (W.Z.)
[2] CNOOC Research Institute Co., Ltd., Beijing 102299, China
* Correspondence: petrocuiyzh@163.com

**Abstract**

The offshore reservoir development involves large injection and production rates and high injection pressures. High-permeability flow channels usually occur in offshore unconsolidated heavy-oil reservoirs during long-term water flux, substantially impacting the production performance. As one important method for identifying channeling, the numerical simulation method with a full-fidelity model is hampered by the low computational efficiency of the history matching process. The GPSNet model is extended for polymer flooding simulations, incorporating complex mechanisms including adsorption and shear-thinning effects, with solutions obtained through a fully implicit numerical scheme. Four flow channel characteristic parameters are proposed, and an evaluation factor *M* for flow channel identification is established with the comprehensive evaluation method. Finally, the field application of the GPSNet model is made and validated by the tracer interpretation result. The history matching speed based on the GPSNet model is 58 times faster than the full-fidelity ECLIPSE model. In addition, the application demonstrates a high degree of consistency with tracer monitoring results, confirming the accuracy and field feasibility. The new method enables rapid and accurate identification and prediction of large and dominant channels, offering effective guidance for targeted treatment of channels and sustainable development of polymer flooding.

**Keywords:** heavy oil; polymer flooding; GPSNet model; history matching; flow channel identification

check for updates

Academic Editor: Vijaya Raghavan

Received: 22 July 2025
Revised: 8 August 2025
Accepted: 12 August 2025
Published: 18 August 2025

**Citation:** Wei, Z.; Cui, Y.; Su, Y.; Zhou, W. Fast History Matching and Flow Channel Identification for Polymer Flooding Reservoir with a Physics-Based Data-Driven Model. *Processes* **2025**, *13*, 2610. https://doi.org/10.3390/pr13082610

**Copyright:** © 2025 by the authors. Licensee MDPI, Basel, Switzerland. This article is an open access article distributed under the terms and conditions of the Creative Commons Attribution (CC BY) license (https://creativecommons.org/licenses/by/4.0/).

## 1. Introduction

Polymer flooding is an essential method to enhance oil recovery [1,2]. Adding water-soluble polymers will increase the viscosity of the water, hence improving mobility control. Hydrolyzed polyacrylamide (HPAM), the popular synthetic polymer, has been successfully implemented in various offshore heavy oil fields, resulting in substantial improvements in oil recovery and reductions in water cut [3,4]. Different from water, a polymer solution exhibits complex mechanisms such as shear-thinning viscosity during experimental studies.

Unconsolidated oil field reservoirs are easily eroded by the water and polymer flux [5,6]. The offshore development process involves high production rates and high injection pressures, which exacerbate erosion effects and lead to high permeability flow channels [7–9]. The existence of high flow channels has serious effects on oil field development since injected water would circulate inefficiently and sweep out of the reservoir

rapidly [10,11]. Unsatisfactory polymer flooding development would be observed with rapid polymer breakthrough. Therefore, the accurate identification of the flow channel becomes an essential task. The tracer test is one of the most convincing methods to identify the flow channels. However, it is expensive and has an influence on the production work. In addition, numerical simulation plays a crucial role in identifying inter-well flow channels [12]. Ding et al. (2016) achieved the identification of the flow channel with numerical simulation and fuzzy method [13]. Nevertheless, traditional full-fidelity numerical simulation history matching is time-consuming with multiple wells and massive grids [14,15]. There is an urgent need to develop rapid polymer flooding numerical simulation technology for the quantitative identification and classification of flow channels.

As a prominent research area, numerous scholars have conducted extensive studies on rapid reservoir simulation technology. Much work has been done on the surrogate model with data-driven and physics-based methods [16,17]. As one of the surrogate methods, the inter-well model, which can directly exhibit the well-to-well connection, shows advantages in flow channel identification studies. Yousef et al. proposed a capacitance-resistance dynamic response method (CRM), which only relies on injection-production dynamics [18,19]. It can obtain the injection-production response intensity between different wells. While this model offers fast calculation speeds, it is relatively simplistic. To address the limitations of CRM, Zhao et al. introduced the inter-well numerical simulation model (INSIM), which simplifies the model to inter-well connections [15,20]. However, in this method, an IMPES solution is adopted. The pressure equation is solved first, with the saturation equation solved afterward. It is hard to extend to cases with complex flow mechanisms for robust simulation, such as polymer flooding. Following this, Lutidze and Younis (2018) developed the StellNet numerical model; the inter-well connection is further divided and adopts a full implicit method for more robust and accurate simulation [21]. Furthermore, Ren et al. (2019) proposed the general-purpose simulator-powered network model (GPSNet) based on the StellNet numerical model [22]. The inter-well connection network construction method is established. Historical matching and optimization are achieved for the long-term water-flooded and steam-flooded reservoirs [23–25]. Further, Wang (2024) extended the GPSNet model to a multi-fractured horizontal well for unconventional fields [26]. In addition, there are many physics-informed machine learning surrogate methods (PIML) that mainly focus on the water flooding process [27,28]. As we know, the flow mechanisms of polymer flooding are more complex than water flooding with shear-thinning viscosity, adsorption, and so on, which pose significant challenges for reservoir simulation. The CRM, INSIM, and PIML models can hardly achieve a stable and accurate flow dynamic simulation for a field case with a hundred wells. However, GPSNet, which is solved with finite volume discretization and the Newton iterative method, can achieve a robust simulation for complex situations. Then, GPSNet is selected for the fast history matching and flow channel identification. While GPSNet models have made significant developments in water flooding, steam flooding, and unconventional reservoir scenarios, there is still a lack of studies for polymer flooding.

Therefore, this study extends the GPSNet model to the polymer flooding simulation with a complex flow mechanism. The main structure of the manuscript is organized as shown in Figure 1. First, the GPSNet model for polymer flooding is established with the well-to-well connection construction, numerical discretization, and Newton iterative method. Afterward, built upon the GPSNet framework, a novel methodology is introduced to determine the flow channels in offshore heavy oil polymer flooding scenarios. Finally, the method is carried out in a real field case and validated with the tracer result.

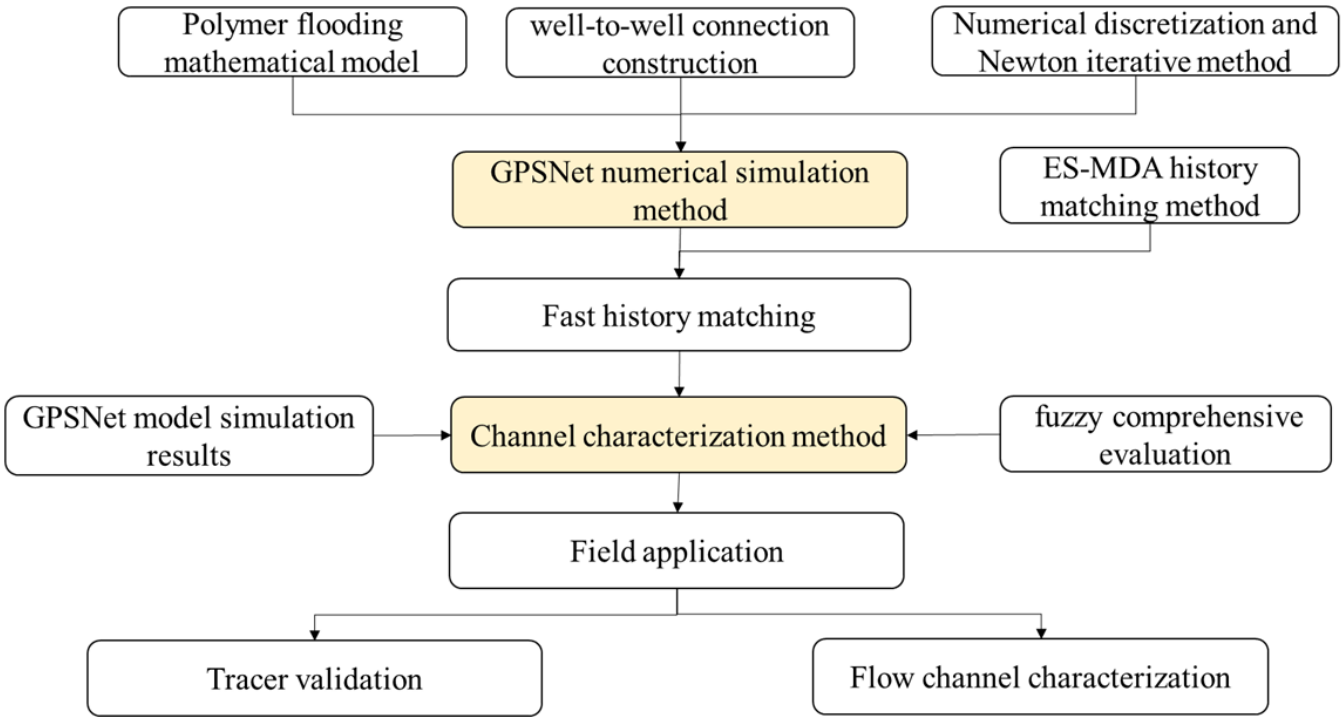



**Figure 1.** The main structure of the manuscript.

## 2. Polymer Flooding GPSNet Model

### *2.1. Polymer Flooding Mathematical Model*

Polymer flooding distinguishes itself from traditional water flooding through several complex physical and chemical mechanisms that are essential for enhanced oil recovery, such as viscosity enhancement, adsorption retention, and reduction in displacement phase permeability. Polymer is assumed to be transported in the aqueous phase in general. Meanwhile, the temperature effect is ignored with the shallow formation in this paper. With the studies of Bao et al. (2017) [27], the mathematical model of polymer flooding is obtained

Water:

$$\frac{\partial}{\partial t}\left(\frac{\phi S_w}{B_w}\right) = \nabla\left[\frac{kk_{rw}}{B_w \mu_{weff} R_k}(\nabla P_w - \rho_w g \nabla z)\right] + q_w \tag{1}$$

Oil:

$$\frac{\partial}{\partial t}\left(\frac{\phi S_o}{B_o}\right) = \nabla\left[\frac{kk_{ro}}{B_o \mu_o}(\nabla P_o - \rho_o g \nabla z)\right] + q_o \tag{2}$$

Polymer:

$$\frac{\partial}{\partial t}\left(\frac{\phi S_w C_p (1 - S_{dpv})}{B_w} + \rho_r C_p^a (1 - \phi)\right) = \nabla\left[\frac{kk_{rw} C_p}{B_w \mu_{peff} R_k}(\nabla P_w - \rho_w g \nabla z)\right] + q_w C_p \tag{3}$$

Permeability reduction:

$$R_k(c, c_{\max}) = 1 + (\mathrm{RRF} - 1)\frac{c^a(c, c_{\max})}{c^a_{\max}} \tag{4}$$

Effective viscosities. The Todd–Longstaff mixing model is adopted to compute the effective viscosities of the water–polymer mixture:

$$\mu_{w,\text{eff}} = \frac{m_\mu(c)^\omega \mu_w}{1 - \bar{c} + \bar{c}/m_\mu(c^*)^{1-\omega}} \tag{5}$$

$$\mu_{p,\text{eff}} = \mu_{fm}(c)^\omega \cdot \mu_p^{1-\omega} \tag{6}$$

where $S_{\text{dpv}}$ represents the non-accessible porosity ratio, dimensionless; $\phi$ denotes porosity, dimensionless; $P_\text{l}$ represents the reservoir pressure, Pa; $k$ stands for the reservoir absolute permeability, $\text{m}^2$; $B_\text{l}$ is the volume coefficient, dimensionless; $S_\text{l}$ represents the saturation, dimensionless; $k_\text{rl}$ is the relative permeability, dimensionless; $\mu_\text{l}$ represent the viscosity, Pa·s; $g$ is the gravity constant, $\text{m/s}^2$; $q_\text{l}$ is the volumes produced or injected per unit volume per unit time, $\text{m}^3/\text{s}$; $C_\text{p}$ is the polymer concentration, $\text{kg/m}^3$; $C_\text{p}{}^\text{a}$ is the adsorbed polymer concentration, kg/kg; $R_\text{k}$ is the permeability reduction coefficient, dimensionless; $\mu_\text{fm}$ denotes the viscosity of a fully mixed polymer solution, Pa·s; $\mu_\text{weff}$ is the effective water viscosity, Pa·s; $\mu_\text{peff}$ is the effective polymer viscosity, Pa·s; $V_\text{b}$ represents the volume of the rock formation, $\text{m}^3$; $\rho_\text{l}$ is the density, $\text{kg/m}^3$; $m_\mu$ represents the viscosity multiplier, dimensionless; *RRF* represents the residual resistance factor, dimensionless; and $l = o, w, r$ represents oil, water, and rock.

### 2.2. GPSNet Model

Based on the idea of inter-well connectivity, the reservoir is simplified into a series of inter-well connections. The generation of the GPSNet follows the original work conducted by Ren et al. (2019) [22]. Firstly, the connection between different wells in which the distances are smaller than the connection maximum length would be established. As we can see in Figure 2, three wells are connected to each other through three connections. Each inter-well connection is assumed to have a constant permeability and further spatially discretized into 10 grids for better simulation accuracy. Then, the grids and connection list of the GPSNet model are obtained. The grid needed for the GPSNet model is reduced by an order of magnitude compared to the full-fidelity simulation. Thus, the computational efficiency would be significantly improved.

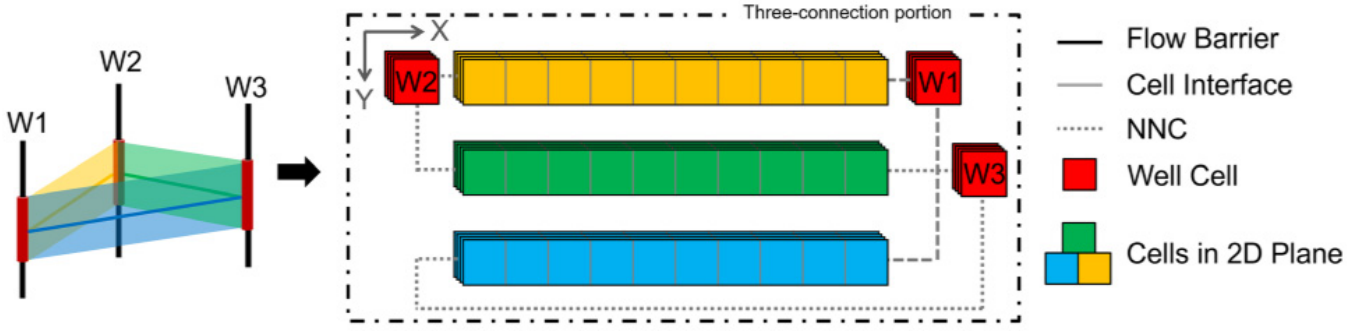



**Figure 2.** A discrete model of each well-to-well connection [22].

Compared to an oil–water two-phase model, the polymer flooding model is more complex. With the implicit pressure and explicit saturation method, it is hard to obtain a stable and accurate result. Then, finite volume and fully implicit methods are adopted. Following the work of Wang et al. (2024) [29], discrete flow equations are obtained based on the form `Div` and `Grad` as the discrete numerical analogs of the standard divergence and gradient operators.

$$\frac{V_b\phi}{\Delta t}\left[\left(\frac{S_o}{B_o}\right)^{n+1}-\left(\frac{S_o}{B_o}\right)^{n}\right]=div(v_o^{n+1})+q_o \tag{7}$$

$$\frac{V_b\phi}{\Delta t}\left[\left(\frac{S_w}{B_w}\right)^{n+1}-\left(\frac{S_w}{B_w}\right)^{n}\right]=div(v_w^{n+1})+q_o \tag{8}$$

$$\begin{aligned}&\frac{V_b\phi}{\Delta t}\left[\left(\frac{S_wC_p(1-S_{dpv})}{B_w}+\rho_rC_p^a(1-\phi)\right)^{n+1}-\left(\frac{S_wC_p(1-S_{dpv})}{B_w}+\rho_rC_p^a(1-\phi)\right)^{n}\right]\\&=div(v_p^{n+1}c_p^{n+1})+q_oc_p\end{aligned} \tag{9}$$

where: $v_o=\frac{kk_{ro}}{B_o\mu_o}(\nabla P_o-\rho_og\nabla z)$, $v_w=\frac{kk_{rw}}{B_w\mu_{weff}R_k}(\nabla P_w-\rho_wg\nabla z)$, $v_p=\frac{kk_{rw}}{B_w\mu_{peff}R_k}(\nabla P_w-\rho_wg\nabla z)$.

Then, the solution of the fully implicit model is obtained using the Newton–Raphson iteration method:

$$\begin{bmatrix}\frac{\partial R_w}{\partial S_w}&\frac{\partial R_w}{\partial P}&\frac{\partial R_w}{\partial c_p}\\\frac{\partial R_o}{\partial S_w}&\frac{\partial R_o}{\partial P}&\frac{\partial R_o}{\partial c_p}\\\frac{\partial R_p}{\partial S_w}&\frac{\partial R_p}{\partial P}&\frac{\partial R_p}{\partial c_p}\end{bmatrix}\begin{vmatrix}\delta S_w\\\delta P\\\delta c_p\end{vmatrix}=\begin{vmatrix}R_w\\R_o\\R_p\end{vmatrix} \tag{10}$$

This approach enables the simultaneous solution of all equations at each time step, thereby achieving stable and robust polymer flooding simulations that incorporate multiple flow mechanisms. Subsequently, stable and significantly accelerated computations of polymer flooding are realized through the utilization of the GPSNet model introduced in this paper.

### *2.3. History Matching Method*

In this study, an ensemble smoother with multiple data assimilation (ES-MDA) is adopted for history matching to the observation data. Following our previous studies, the ensemble smoother with multiple data assimilation performs data assimilation $N_s$ times ($N_s > 1$) for all observation data with uniform or adaptive multiplication coefficients [30].

Given a model m and observation data d, the analysis equation yields the following:

$$m_g^{n+1}=m_g^n+C_{MD}^n(C_{DD}^n+\alpha_nC_D)^{-1}\left(d_{uc,g}^n-d_g^n\right)\ g=1,2,\ldots,N_e,\ n=1,2,\ldots,N_s \tag{11}$$

where $g$ denotes an arbitrary member of $Ne$ ensembles; $n$, $n+1$ is the current and forecast assimilation step of the $Ns$ steps; $d^n{}_{uc,g}$ is the vector of 'perturbed' observations; $d^n{}_g$ vector of predicted data; $C_{MD}{}^n$ is the cross-covariance matrix between the prior vector of model parameters $m^n{}_g$ and the vector of predicted data $d^n{}_g$; $C_{DD}{}^n$ is the autocovariance matrix of predicted data $d_g$; $C_D$ is the covariance matrix of measurement error for $d_g$; and $a_n$ is the inflating factor.

## 3. Flow Channel Characterization Method

As a hot research topic, much work has been done on the flow channel characterization. It has been found that the flow channel occurrence is highly related to the permeability ratio, water cut, and displacement ratio. Additionally, the fuzzy comprehensive evaluation (FCE) method is identified as an effective method for flow channel characterization. Then, based on the studies of Ding et al., 2016 [13], flow channel characterization key parameters

based on the GPSNet model are proposed; then, the flow channel characterization method is established using the fuzzy comprehensive evaluation (FCE) method.

### 3.1. Channel Characterization Key Parameters

With long-term water flooding, the sand in unconsolidated reservoirs begins to move, leading to the formation of flow channels with high permeability in the reservoir. These high-permeability flow channels subsequently become the primary conduits for fluid flow, significantly influencing production performance. The occurrence of flow channels is closely related to the strength of water flooding and the properties of the rock.

In this study, we identify four key parameters influencing flow channel development: reservoir permeability, water injection volume ratio, water injection efficiency, and the rise rate of water cut. Higher permeability signifies enhanced flow capacity and increased water flux. Similarly, a larger injection volume ratio correlates with a heightened channel development probability. When flow channels are present around the production well, lower injection efficiency and a more rapid increase in water cut are observed.

These parameters, including permeability, water injection volume ratio, water injection efficiency, and water cut rise rate, can be calculated from the parameter inversion results of the GPSNet model.

Permeability $K_{ij}$: The permeability of the inter-well connection, mD.

Water injection volume ratio ($R_{ij}$): the ratio of the injected amount $q_{inj}$ to the connected volume:

$$R_{ij} = \frac{q_{inj}}{V_{ij}} \tag{12}$$

Water injection efficiency $E_{w,ij}$:

$$E_{w,ij} = \frac{q_o}{q_{inj}} \tag{13}$$

Water cut rise rate $V_{w,ij}$:

$$V_{w,ij} = \frac{fw_{ij,t} - fw_{ij,t_0}}{t - t_0} \tag{14}$$

where $V_{ij}$ is the reservoir porosity volume between the $i$-th injection well and the $j$-$th$ production wells, $m^3$; $q_o$ is oil production rate, $m^3$/month; $q_{inj}$ is injection rate, $m^3$/d; and $f_{wij,t}$ is the water cut at time $t$, dimensionless.

### 3.2. Channel Characterization Method

Based on the four characteristic parameters, the flow channels characterization method is developed using the fuzzy comprehensive evaluation (FCE) method [13]. First, the four characteristic parameters are normalized with the trapezoidal membership function.

$$N_{k,ij} = \frac{K_{ij} - K_{ij,\min}}{K_{ij,\max} - K_{ij,\min}} \tag{15}$$

$$N_{R,ij} = \frac{R_{ij} - R_{ij,\min}}{R_{ij,\max} - R_{ij,\min}} \tag{16}$$

$$N_{EW,ij} = \frac{E_{w,ij,\max} - E_{w,ij}}{E_{w,ij,\max} - E_{w,ij,\min}} \tag{17}$$

$$N_{VW,ij} = \frac{V_{w,ij} - V_{w,ij,\min}}{V_{w,ij,\max} - V_{w,ij,\min}} \tag{18}$$

where $N_{ij}$ is the membership degree of the $j$-th objective index of factor $i$, which is also the standardized measurement value, the subscript max is the maximum value, and the subscript min is the minimum value.

Based on normalization, the comprehensive evaluation factor $M_{ij}$ of channeling intensity is established with the fuzzy comprehensive evaluation (FCE) method:

$$M_{ij} = N_{k,ij} \cdot w_1 + N_{R,ij} \cdot w_2 + N_{EW,ij} \cdot w_3 + N_{VW,ij} \cdot w_4 \quad (19)$$

where $w_1$, $w_2$, $w_3$, and $w_4$ are the corresponding weights. Applying this method, a classification threshold for channeling intensity in offshore heavy oil fields is established using the parameters in Table 1. As shown in Table 2, channels with $M$ values exceeding 0.65 are classified as large channels; those within the range of 0.55 to 0.65 are deemed advantageous channels, and values below 0.55 indicate a non-channel development. By establishing these grading criteria, we offer a clear and systematic approach to identifying the flow channels in offshore heavy oil fields.

**Table 1.** The values of the corresponding weight.

| Parameters | $w_1$ | $w_2$ | $w_3$ | $w_4$ |
|---|---|---|---|---|
| Value | 1 | 3 | 5 | 5 |

**Table 2.** Classification table of channeling channels of offshore heavy oil polymers.

| $M$ | Channeling Intensity Grading |
|---|---|
| >0.65 | Large channel |
| 0.55~0.65 | Advantageous channel |
| <0.55 | Not developing |

## 4. Field Application

The S oil field features an average permeability of 2000 mD, with the underground crude oil exhibiting an average viscosity of 88 mPa·s, both indicative of a typical heavy oil field offshore. The oil field was put into operation in 1994, with 103 production wells and 40 water injection wells. In 2008, polymer flooding was fully implemented, with a total of 24 injection wells, and an evident improvement in oil recovery was observed with polymer flooding. However, a high rate of water cut rise was observed in production wells during the development, suggesting the presence of high-permeability flow channels. The presence and characteristics of the flow channels determine the production performance. It is essential to identify the flow channels between different wells. In this part, the GPSNet model and channel characterization method are utilized in this field.

### *4.1. Field History Matching*

History matching and flow channel identification are carried out in the S oil field. First, the GPSNet inter-well communication network structure of the S oil field was constructed as shown in Figure 3. We can see that the 3D full numerical model was simplified into connections between different wells, each further divided into ten grids for better simulation performance.

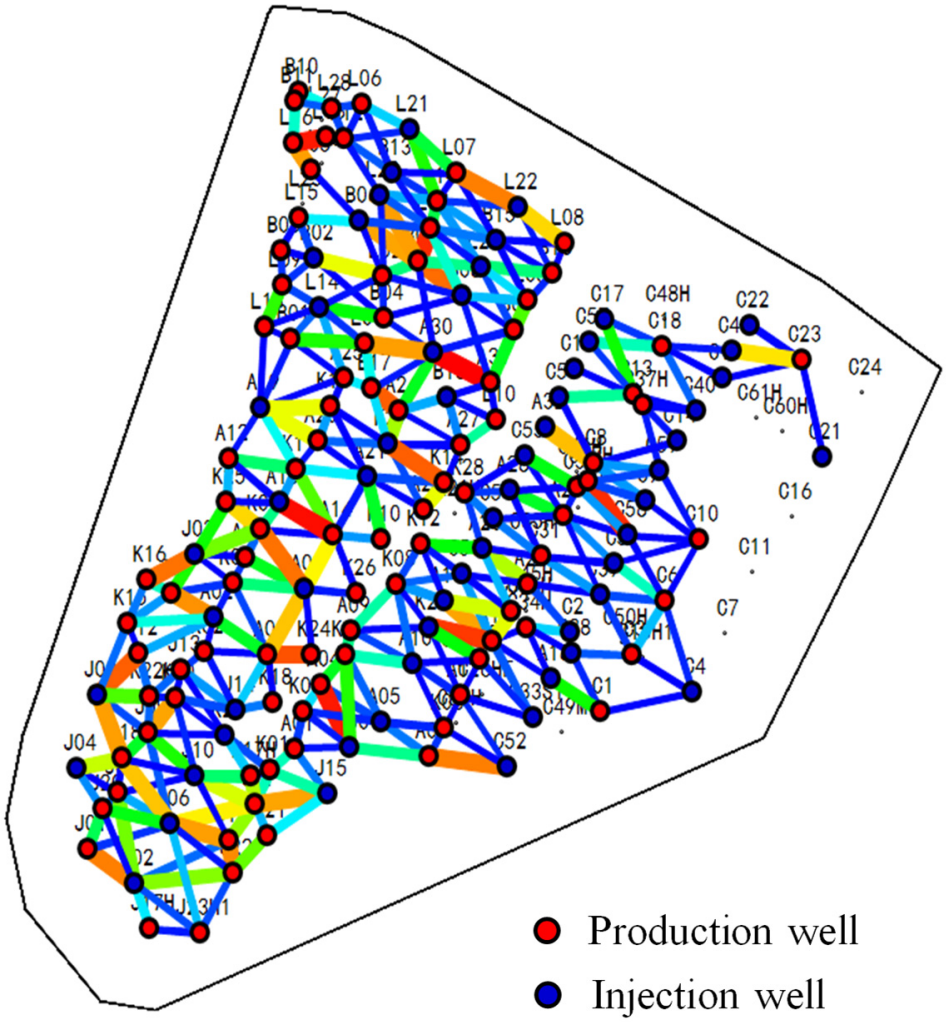



**Figure 3.** GPSNet model of the actual reservoir (blue represents the injection well; red represents the production well).

In this work, 22 years (January 2022–March 2024) of historical data are used to calibrate the GPSNet model. A monthly allocation of well-level injection and production historical data is available for the period under investigation, taking reservoir properties as uncertainty parameters within ranges guided by geology and available data. Subsequently, historical fitting work was conducted using the ES-MDA method with $N_s$ = 4 and $N_e$ = 100.

The fitting results of the production data for the S oil field and some single wells are depicted in Figures 4–6. Figure 6 shows the fitting results of the polymer concentration of two production wells. Notably, the simulation results closely align with the field production data, with a dynamic fitting error of approximately 5% for the entire field production dynamic and a fitting error of about 10% for single wells, as shown in Figure 7. Furthermore, compared to the time consumption of the traditional ECLIPSE model (46.1 h), polymer flooding simulation based on the GPSNet model requires only 0.8 h, resulting in a calculation speed 58 times faster. These findings show the applicability of the GPSNet model for real polymer flooding fields.

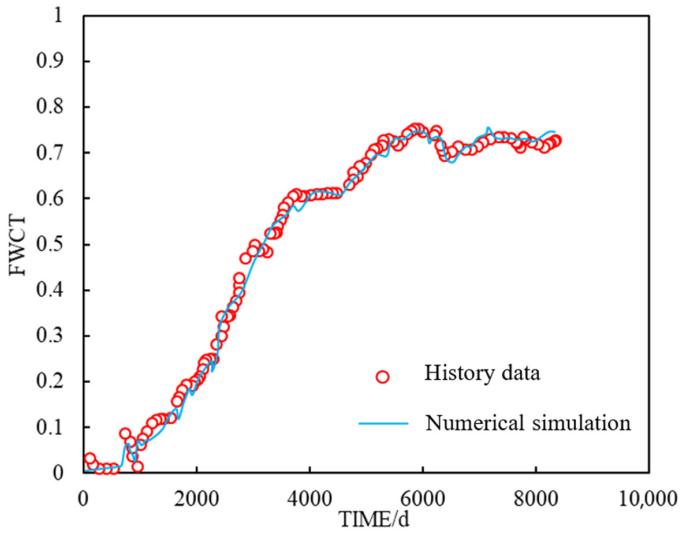



**Figure 4.** Fitting results of the water cut of the oil field.

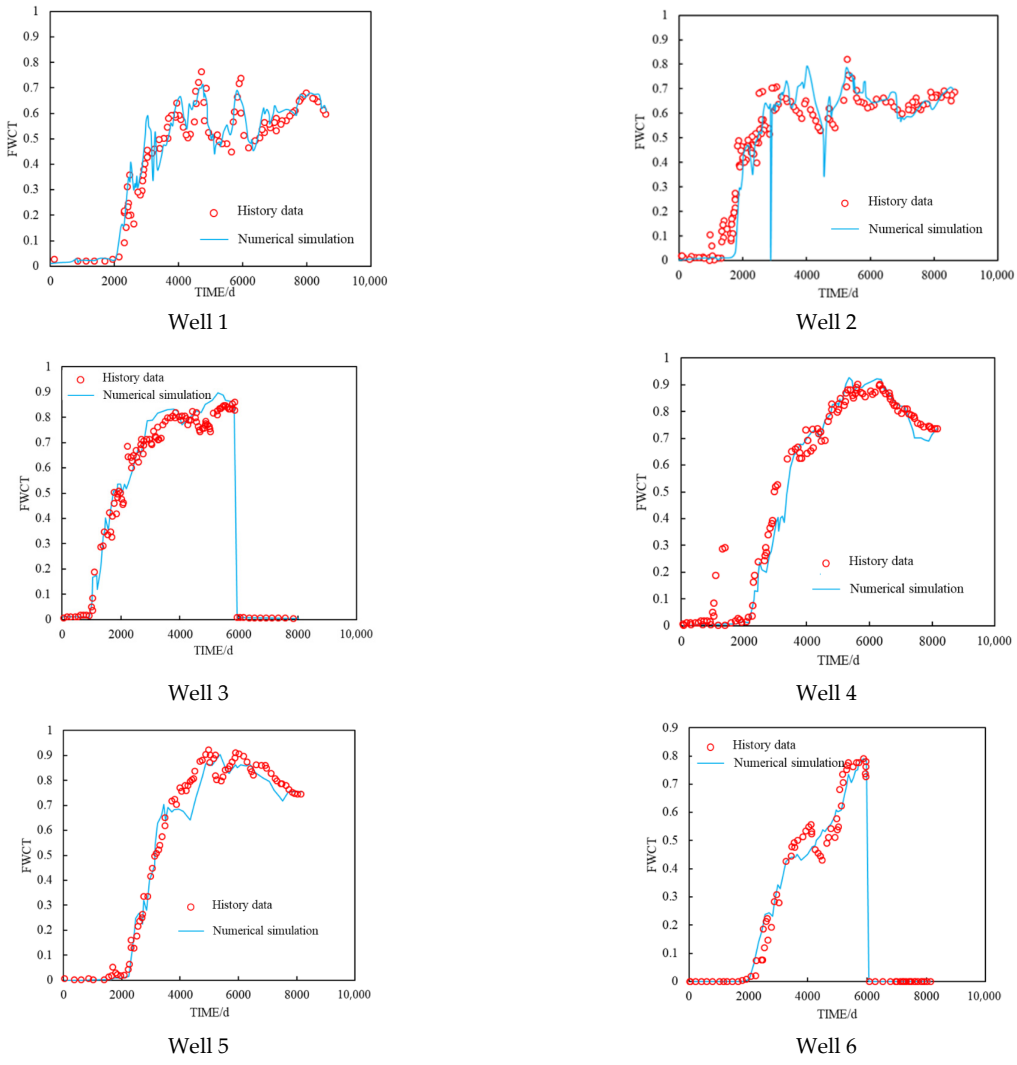



**Figure 5.** Fitting results of the water cut of six production wells.




Well 7 Well 8

**Figure 6.** Fitting results of the two production wells' polymer production concentration.

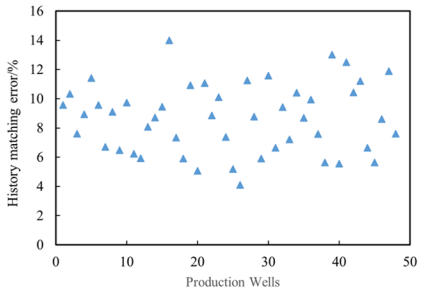



**Figure 7.** Fitting errors of production wells.

### *4.2. Quantification of Flow Channels*

After the history matching with the GPSNet model, the characterization of flow channels was conducted and validated with the tracer interpretation results.

In June 2021, a tracer test was conducted for reservoir characterization. Taking well A08 as an example, the tracer injected into the Id section of well A08 was detected in well A14 after 28 days, with an initial concentration of 6.23 μg/L. The flow rate of the water injection front was measured at 10.7 m/d, leading to an interpreted permeability of 10,624 mD with the tracer data. Additionally, the tracer test interpretation results for J14 and A02 are also presented in Table 3.

**Table 3.** The channel characterization validation of the new method with the tracer test.

| Well | Formation | The New Method | | | | | | | Tracer Method | |
|---|---|---|---|---|---|---|---|---|---|---|
| | | Injection Ratio, (104·d)-1 | Injection Efficiency, $m^3/m^3$ | Rate of Water Cut Increase, Month-1 | Comprehensive Judging Factor | Corresponding Production Wells | Permeability/mD | Identify the Results | The Tracer Interprets the Results | Permeability/mD |
| A02 | Iu | 35.10 | 0.01 | 0.446 | 0.59 | J12 | 7900 | Advantageous channel | Large flow channel | 8750 |
| | Id | 71.48 | 0.02 | 0.838 | 0.83 | K04 | 9860 | Large flow channel | Large flow channel | 10,500 |
| A08 | Id | 24.40 | 0.01 | 0.817 | 0.78 | A14 | 12,430 | Large flow channel | Large flow channel | 10,624 |
| | II | 69.32 | 0.02 | 0.82 | 0.82 | A07 | 10,970 | Large flow channel | Large flow channel | 11,058 |
| J14 | Iu | 9.42 | 0.04 | 0.635 | 0.67 | J13 | 11,270 | Large flow channel | Large flow channel | 12,350 |
| | Id | 24.40 | 0.04 | 0.565 | 0.62 | K20 | 7530 | Advantageous channel | Advantageous channel | 7960 |

On the basis of the history matching fitting results, the comprehensive characterization factor M is determined for each injection and production direction, as detailed in Table 2. It is evident that the channel identification results obtained with this new method closely agree with the tracer interpretation results, thus validating the accuracy of the method proposed in this paper. Moreover, compared to the tracer method, the new approach

enables rapid and accurate identification of the development of large pores and dominant channels, without disrupting normal production operations.

After the new channel characterization method was validated, it was applied to channel characterization for other wells. As shown in Table 4 and Figure 8, we can see that large flow channels were identified from J08 to K15. Four advantageous channels were found in J03, J10, K23, J08, and J06 of the Id formation.

**Table 4.** The channel characterization of the new method.

| Well | Formation | Comprehensive Judging Factor, M | Corresponding to Production Wells | Identify the Results |
|---|---|---|---|---|
| J03 | Iu | 0.58 | A07 | Advantageous channel |
| | Id | 0.61 | K16 | Advantageous channel |
| J10 | Iu | \ | \ | \ |
| | Id | 0.59 | K20 | Advantageous channel |
| K23 | Iu | 0.49 | K20 | \ |
| | Id | 0.57 | K17H | Advantageous channel |
| J08 | Iu | \ | \ | \ |
| | Id | 0.81 | K15 | Large flow channel |
| J06 | Iu | \ | \ | \ |
| | Id | 0.60 | J05 | Advantageous channel |

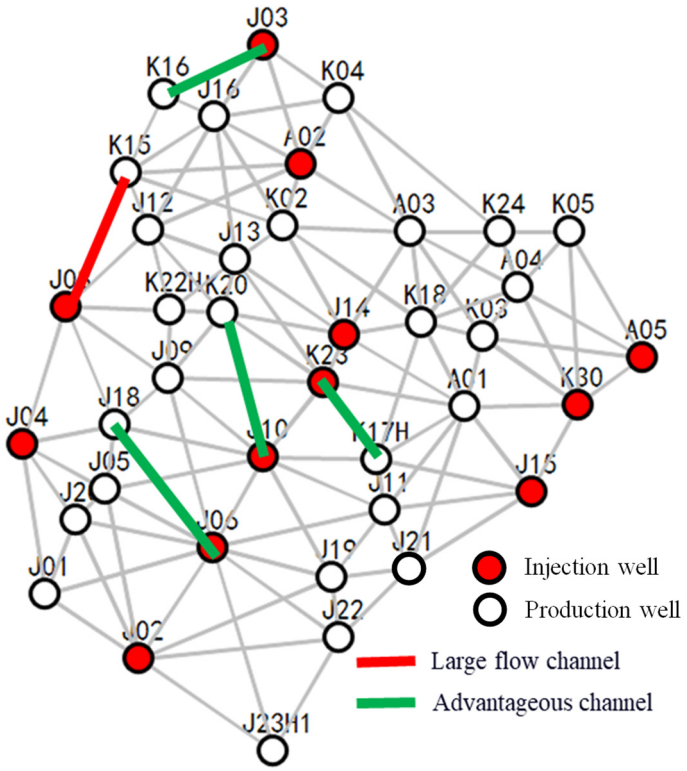



**Figure 8.** The flow channel characterization result.

## 5. Conclusions

In this paper, a GPSNet model is established for the fast and accurate flow channel identification of polymer flooding based on the history matching process. The method is

carried out in one field application and validated. It is applicable for oil fields with a long production history. With this model, the following conclusions can be drawn:

(1) The GPSNet model achieves a stable polymer flooding simulation incorporating the complex flooding mechanism with a fully implicit method. In this model, the three-dimensional full-grid model is simplified into a connectivity network model between injection and production wells. This GPSNet polymer flooding model demonstrates a significant improvement in calculation speed, with it being more than 50 times faster than the conventional full-grid numerical simulation method.

(2) The comprehensive evaluation factor $M$ is established based on inter-well permeability, water injection volume ratio, water injection efficiency, and water cut rise rate. The threshold for different flow channels in one offshore heavy oil field $S$ is proposed. The $M$ greater than 0.65 indicates a large channel, while $M$ values falling between 0.55 and 0.65 represent an advantageous channel. The results obtained with this new method closely align with tracer interpretation results, affirming the accuracy of the method proposed in this paper.

(3) The new method can quickly and accurately identify the development of dominant channels, without affecting normal production. More application in offshore polymer flooding reservoirs is recommended. Furthermore, the method proposed in this paper should be extended to other situations, such as $CO_2$ flooding for the flow channels identification.

**Author Contributions:** Writing—original draft, Y.C.; methodology, Y.S. and W.Z.; data curation and software, Z.W. All authors have read and agreed to the published version of the manuscript.

**Funding:** This research was funded by the National Natural Science Foundation of China (Grant No. 52074347) and the Science and Technology Major Project of CNOOC during the 14th Five-Year Plan (Grant No. KJGG2021-0506).

**Data Availability Statement:** Data are contained within the article.

**Conflicts of Interest:** The authors were all employed by the company CNOOC Research Institute Ltd. The authors declare that the research was conducted in the absence of any commercial or financial relationships that could be construed as a potential conflict of interest.

## References

1. Wang, L.; Zhang, G.C.; Ge, J.-J.; Li, G.H.; Zhang, J.; Ding, B.D. Preparation of microgel nanospheres and their application in EOR. In Proceedings of the SPE International Oil and Gas Conference and Exhibition in China, Beijing, China, 8–10 June 2010; p. SPE-130357.
2. Scott, A.J.; Romero-Zerón, L.; Penlidis, A. Evaluation of polymeric materials for chemical enhanced oil recovery. *Processes* **2020**, *8*, 361. [CrossRef]
3. Cui, Y.; Zhou, W.; Liu, C. Integrated Modeling of Time-Varying Permeability and Non-Darcy Flow in Heavy Oil Reservoirs: Numerical Simulator Development and Case Study. *Processes* **2025**, *13*, 1683. [CrossRef]
4. Jiang, R.; Zhang, W.; Zhao, P.; Jiang, Y.; Cai, M.; Tao, Z.; Zhao, M.; Ni, T.; Xu, J.; Cui, Y.; et al. Characterization of the reservoir property time-variation based on 'surface flux' and simulator development. *Fuel* **2018**, *234*, 924–933. [CrossRef]
5. Yang, R.; Jiang, R.; Guo, S.; Chen, H.; Tang, S.; Duan, R. Analytical study on the Critical Water Cut for Water Plugging: Water cut increasing control and production enhancement. *Energy* **2021**, *214*, 119012. [CrossRef]
6. Lin, J.; Jiang, R.; Shen, Z.; Wang, Q.; Cui, Y.; Ni, Q.; Zhang, F. Comprehensive characterization investigation of multiple time-varying rock-fluid properties in waterflooding development. *J. Energy Resour. Technol.* **2022**, *144*, 073001. [CrossRef]
7. Kamal, M.S.; Sultan, A.S.; Al-Mubaiyedh, U.A.; Hussein, I.A. Review on polymer flooding: Rheology, adsorption, stability, and field applications of various polymer systems. *Polym. Rev.* **2015**, *55*, 491–530. [CrossRef]
8. Song, K.; Tao, J.; Lyu, X.; Xu, Y.; Liu, S.; Wang, Z.; Liu, H.; Zhang, Y.; Fu, H.; Meng, E.; et al. Recent advances in polymer flooding in China. *Molecules* **2022**, *27*, 6978. [CrossRef]
9. Seright, R.S. Potential for polymer flooding reservoirs with viscous oils. *SPE Reserv. Eval. Eng.* **2010**, *13*, 730–740. [CrossRef]
10. Amirian, E.; Dejam, M.; Chen, Z. Performance forecasting for polymer flooding in heavy oil reservoirs. *Fuel* **2018**, *216*, 83–100. [CrossRef]

11. Saboorian-Jooybari, H.; Dejam, M.; Chen, Z. Heavy oil polymer flooding from laboratory core floods to pilot tests and field applications: Half-century studies. *J. Pet. Sci. Eng.* **2016**, *142*, 85–100. [CrossRef]
12. Zhong, D.; Zhu, X. Characteristics and controlling factors of high capacity channels of reservoirs at high water cut stage: A case from Block Hu 12 of Huzhuangji Oilfield. *Pet. Explor. Dev.* **2007**, *34*, 207.
13. Ding, S.; Jiang, H.; Liu, G.; Sun, L.; Lu, X.A.; Zhao, L. Determining the levels and parameters of thief zone based on automatic history matching and fuzzy method. *J. Pet. Sci. Eng.* **2016**, *138*, 138–152. [CrossRef]
14. Peng, S.; Shi, Y.; Han, T.; Yao, T.; Huang, J.; Li, H.; Li, X.; Hu, H. A quantitative description method for channeling-path of reservoirs during high water cut period. *Acta Pet. Sin.* **2007**, *28*, 79.
15. Zhao, H.; Kang, Z.; Zhang, Y.; Sun, H.; Li, Y. An interwell connectivity numerical method for geological parameter characterization and oil-water two-phase dynamic prediction. *Acta Pet. Sin.* **2014**, *35*, 922.
16. Latrach, A.; Malki, M.L.; Morales, M.; Mehana, M.; Rabiei, M. A critical review of physics-informed machine learning applications in subsurface energy systems. *Geoenergy Sci. Eng.* **2024**, *239*, 212938. [CrossRef]
17. Huang, F.; Xiong, H.; Chen, S.; Lv, Z.; Huang, J.; Chang, Z.; Catani, F. Slope stability prediction based on a long short-term memory neural network: Comparisons with convolutional neural networks, support vector machines and random forest models. *Int. J. Coal Sci. Technol.* **2023**, *10*, 18. [CrossRef]
18. Yousef, A.A.; Gentil, P.; Jensen, J.L.; Lake, L.W. A capacitance model to infer interwell connectivity from production-and injection-rate fluctuations. *SPE Reserv. Eval. Eng.* **2006**, *9*, 630–646. [CrossRef]
19. Holanda, R.W.; Gildin, E.; Jensen, J.L.; Lake, L.W.; Kabir, C.S. A state-of-the-art literature review on capacitance resistance models for reservoir characterization and performance forecasting. *Energies* **2018**, *11*, 3368. [CrossRef]
20. Zhao, H.; Yao, J.; Lue, A.M.; Wang, W. Reservoir interwell dynamic connectivity inversion based on injection and production data. *Zhongguo Shi You Daxue Xuebao J. China Univ. Pet. Ed. Nat. Sci.* **2010**, *34*, 91–94.
21. Lutidze, G. StellNet: Physics-Based Data-Driven General Model for Closed-Loop Reservoir Management. Ph.D. Thesis, The University of Tulsa, Tulsa, OK, USA, 2018.
22. Ren, G.; He, J.; Wang, Z.; Younis, R.M.; Wen, X.H. Implementation of physics-based data-driven models with a commercial simulator. In Proceedings of the SPE Reservoir Simulation Conference, Galveston, TX, USA, 10–11 April 2019.
23. Lie, K.A.; Krogstad, S. Comparison of two different types of reduced graph-based reservoir models: Interwell networks (GPSNet) versus aggregated coarse-grid networks (CGNet). *Geoenergy Sci. Eng.* **2023**, *221*, 111266. [CrossRef]
24. Wang, Z.; Guan, X.; Milliken, W.; Wen, X.H. Fast history matching and robust optimization using a novel physics-based data-driven flow network model: An application to a Steamflood sector model. *SPE J.* **2022**, *27*, 2033–2051. [CrossRef]
25. Guan, X.; Wang, Z.; Kostakis, F.; Ren, G.; Guo, G.; Milliken, W.J.; Rangaratnam, B.; Wen, X.H. Fast history matching and optimization using a novel physics-based data-driven model: An application to a diatomite reservoir with hundreds of wells. *Geoenergy Sci. Eng.* **2023**, *228*, 211919. [CrossRef]
26. Wang, Z. A fast physics-based data-driven surrogate model for unconventional reservoirs with rapid decline and well interference. *Geoenergy Sci. Eng.* **2024**, *237*, 212772. [CrossRef]
27. Bao, K.; Lie, K.A.; Møyner, O.; Liu, M. Fully implicit simulation of polymer flooding with MRST. *Comput. Geosci.* **2017**, *21*, 1219–1244. [CrossRef]
28. Bi, J.; Li, J.; Wu, K.; Chen, Z.; Chen, S.; Jiang, L.; Feng, D.; Deng, P. A physics-informed spatial-temporal neural network for reservoir simulation and uncertainty quantification. *SPE J.* **2024**, *29*, 2026–2043. [CrossRef]
29. Wang, H.; Wang, M.; Chen, S.; Hui, G.; Pang, Y. A novel governing equation for shale gas production prediction via physics-informed neural networks. *Expert Syst. Appl.* **2024**, *248*, 123387. [CrossRef]
30. Emerick, A.A.; Reynolds, A.C. Ensemble smoother with multiple data assimilation. *Comput. Geosci.* **2013**, *55*, 3–15. [CrossRef]


**Disclaimer/Publisher's Note:** The statements, opinions and data contained in all publications are solely those of the individual author(s) and contributor(s) and not of MDPI and/or the editor(s). MDPI and/or the editor(s) disclaim responsibility for any injury to people or property resulting from any ideas, methods, instructions or products referred to in the content.